

# Lithography Techniques Using Local-Probe Microscopy

## 3.1. Introduction

About twenty years ago, a new category within the field of nanolithography techniques was created by the introduction of local-probe microscopes [SAL 99, WIE 94], which take advantage of the local interaction that exist between a probe and the surface to be patterned. There is a whole family of such microscopes, the best known being scanning tunneling microscopes (STMs) [BIN 82], and atomic force microscopes (AFMs) [BIN 86] (Figure 3.1). Their fame is such that they are sometimes considered to be the workhorses of nanotechnology. We are going to show in this chapter that these microscopes, thanks to their ultimate resolution, can be viewed as the “end of the roadmap” of top-down techniques for nanolithography. Indeed, their resolution makes it possible to not only resolve but also to provide precise imaging of the elementary constituents of matter (atoms, molecules), and they were soon recognized as valuable tools for patterning with atomic resolution.

Since their advent in the late 80s, their importance has grown rapidly, notably when used in combination with complementary techniques involving bottom-up approaches, such as self-assembly, guided growth, chemical reactions etc. They are at the crossroads of the two “top-down” and “bottom-up” approaches and are also compatible with a great number of analytical tools (optical, electrochemical etc.). Scanning probe techniques are therefore bound to play a central role in the nanofabrication evolution of the next decades.

---

Vincent BOUCHIAT , Néel Institute , CNRS-Grenoble

### 3.2. Presentation of local-probe microscopes

Although each tool differs according to the detail of its mechanism, local probe microscopes all share the same principle: a local probe (referred to, for the rest of this chapter, as a ‘tip’) is brought close to a sample, down to a nanometric distance from the surface, and the local physical properties (electrical, optical, mechanical, etc.) that result from the tip–sample interaction are measured in real-time. This measurement of this “near-field” interaction makes it possible to control the position of the tip in relation to the surface and to record information about its local properties (topography, conductance, chemical composition, etc.); see Figure 3.1.

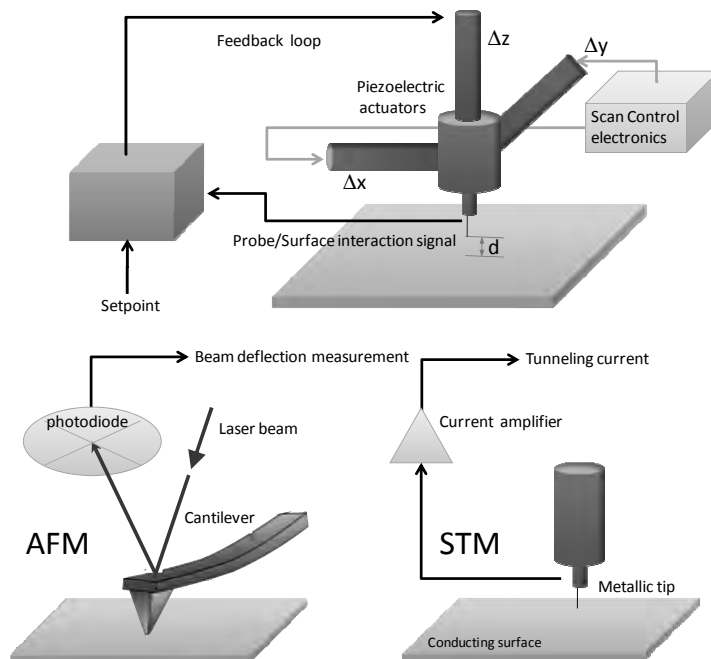


**Figure 3.1.** General principle of operation of local-probe microscopes: the position of the tip is controlled in three directions by means of piezoelectric tubes. The continuous measurement of the probe/sample interaction signal allows the real-time control of the vertical position  $d$  of the probe while scanning in the  $X$  and  $Y$  directions. The topographic image results from the recording of  $Z(X, Y)$ . Bottom, left: AFM microscopy principle: the interaction signal is the deflection of a laser beam focused on a cantilever on which a tip is attached. Bottom, right: STM microscopy principle: the interaction signal is the measurement of the tunnel current between the tip and the surface of the conducting surface.

The relative position of the tip with respect to the surface is controlled by applying high voltages on piezoelectric ceramics (so-called ‘scanners’) that can move in three directions thanks to the application of an electronic voltage at their end. In this way, they ensure the accuracy of the distances  $\Delta x$ ,  $\Delta y$  and  $\Delta z$  to better than one angström, meaning that they have the ability to resolve the inter-atomic distances when placed in a suitable environment (an ultra-high vacuum).

In the case of atomic force microscopy (AFM), the interaction potential between the atoms of the end of the tip and those at the sample surface generates a local force, the gradient of which at distance  $d$  is extremely high. This force is measured thanks to the deflection of a laser beam focused on the reverse side of a mechanical cantilever on which the tip is attached. In the case of scanning tunneling microscopy (STM), the electronic current, resulting from electrons tunneling between the metallic tip and the surface, is amplified and then measured. The regulation of this current allows the electronic density to be recorded and imaged while the tip scans the surface.

In the case of Near-field Scanning Optical microscopes (NSOMs) [HEI 94], the evanescent electromagnetic wave generated at the tip-sample gap is collected at a distance shorter than the wavelength by means of an adapted optical system (fiber, etc.). To summarize, local-probe microscopes achieve the imaging of a surface by measuring a physical quantity in a non-propagative regime (hence the name “near-field” interaction). Depending on which microscope is used, this can be a tunnel effect current, an attractive or repulsive force, or an evanescent electromagnetic wave.

### 3.3. General principles of local-probe lithography techniques

The principles of scanning probe lithography techniques [AMP 05] are based on a simple idea: since these microscopes make it possible to achieve an image of the surface at the nanometric or even at the atomic scale, why not use them to modify a surface at the same scale?

The local interaction between the tip and the surface can indeed be used to modify a surface in a permanent way, according to a predefined lithographic pattern. The first applications [ALB 89, EIG 90] of these simple principles were demonstrated a few years after the invention of these microscopes. In the case of scanning tunneling microscopes, because the substrate needs to be conducting, the manipulation is most often achieved by changing the electrical conditions under which the tip is operated (the voltage pulse applied on the tip, modification of the regulation set point, etc.).

It is important to realize that scanning probe microscopes only provide surface imaging and cannot “see” below the surface. The absence of “lenses” (i.e. focusing elements) makes the tip-surface interaction diverge rapidly with depth. Consequently, they are not well adapted for in-depth structuring of a volume. The lithographic processes developed from these microscopes must take into account this issue. The structures readily produced after lithography will not have an aspect ratio (defined as the ratio of height/width of a pattern) above unity and only shallow nanostructuring can be envisioned. However, as seen in the following sections, specific physico-chemical methods can be used to “amplify” an ultra-thin lithographic pattern and allow that pattern to be transferred to the underlying layer without a significant increase of line width.

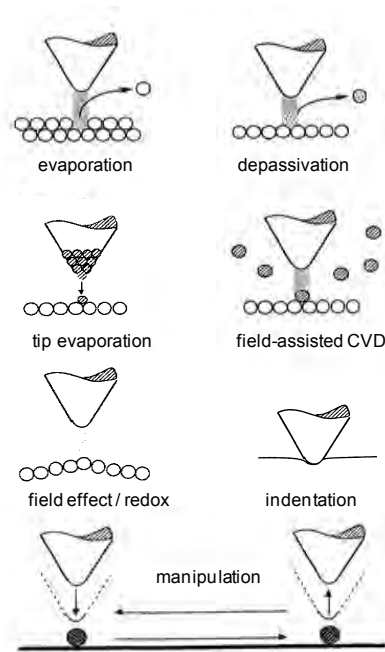


**Figure 3.2.** Schematics of the different types of surface modification induced by local-probe microscope tips. Examples of the physical principles involved are described in the following sections of this chapter

### 3.4. Classification of surface structuring techniques using local-probe microscopes

A peculiarity of scanning probe microscopes is that their resolution is of the same order of magnitude as that of matter's elementary constituents (atoms, molecules, etc.). Consequently, patterning can take into account its discontinuous and discrete nature and enable manipulation of the nano-objects one by one, leading to the direct fabrication of devices exhibiting quantum properties (Figure 3.3 and 3.4).

The ultimate challenge of the fabrication of a structure controlled atom by atom was taken up as early as 1990 by pioneering teams [ALB 89, EIG 90] specializing in scanning tunneling microscopy under ultra-high vacuums. Their work culminated, in 1993, with the demonstration of artificially made structures such as “quantum corrals” [CRO 93] that show the confinement of electron waves (see Figure 3.3). Subsequently, a large number of different techniques have been suggested to nanometrically modify a surface (atom or molecule manipulation, controlled evaporation of atoms [LEB 97], indentation, resist insulation, local oxidation, etc.).

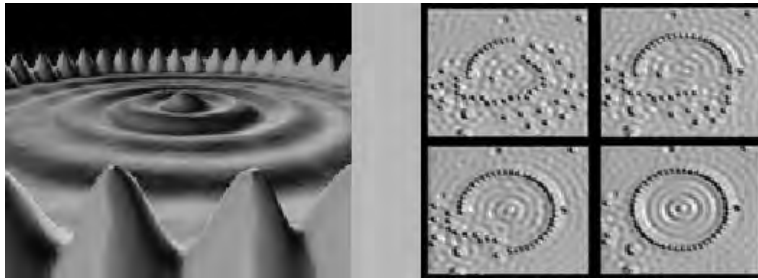


**Figure 3.3.** Manipulation of adsorbed xenon atoms on a copper surface using a scanning tunneling microscope under high vacuum and at low temperature. The artificial structure is a 7nm wide Xenon ring created by atom-per-atom manipulation using the tip of the microscope as a grabbing tool. The standing waves within the ring correspond to electronic standing waves induced on the copper metallic surface by scattering of the Xenon atoms. The artificially-produced ring, which has been named “quantum corral”, is an illustration of the confinement of these waves. The resonance of the electromagnetic wave imposed by the conditions at the limits is more significant at the center of the ring when it is closed. Adapted from [CRO 93]; Figure © IBM

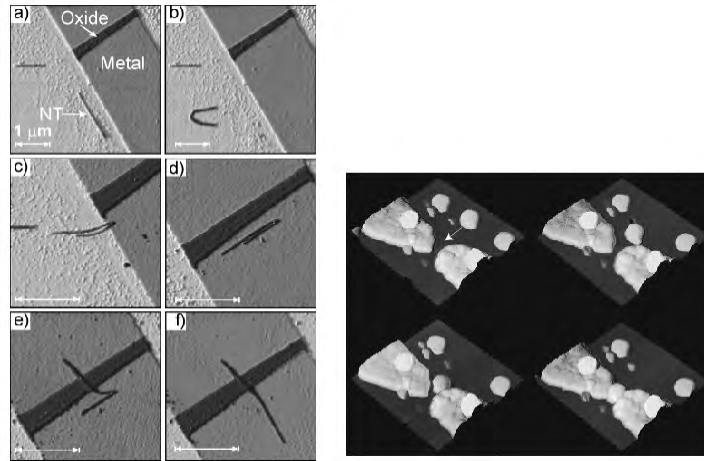


**Figure 3.4.** Series of atomic force micrographs showing manipulation of carbon nanotubes (left, taken from [AVO 99] ) and a gold particle (right, taken from [JUN 98]). In both cases, the nano-object (carbon nanotube left, gold nanoparticle right) is manipulated using an AFM tip. The nano-object eventually bridges the two electrodes, creating an active device which exhibits quantum properties

#### 3.4.1. Classification according to the physical nature of the interaction

Except for the two cases described in section 3.7 below, for which the tip plays a passive role in positioning, all the lithographies are based on the energetic interactions between the tip and the modified surface. The microscope's tip thus acts as a punctual energy source which can have having different physical actions: electrical, mechanical, optical or thermal.

It is then possible to classify most of the lithography techniques with respect to the physical origin of the interaction responsible for the surface modification (see Figure 3.5). Each type of interaction has led to several lithography techniques depending on the materials involved, thus creating a classification tree. Some of the applications have remained at the prototype stage, whereas others have reached an advanced pre-industrial state. One of the latter, for example, involves the high-speed thermo-mechanical indentation of resists [VET 00]. This technique, developed by IBM is a promising technique for information storage.

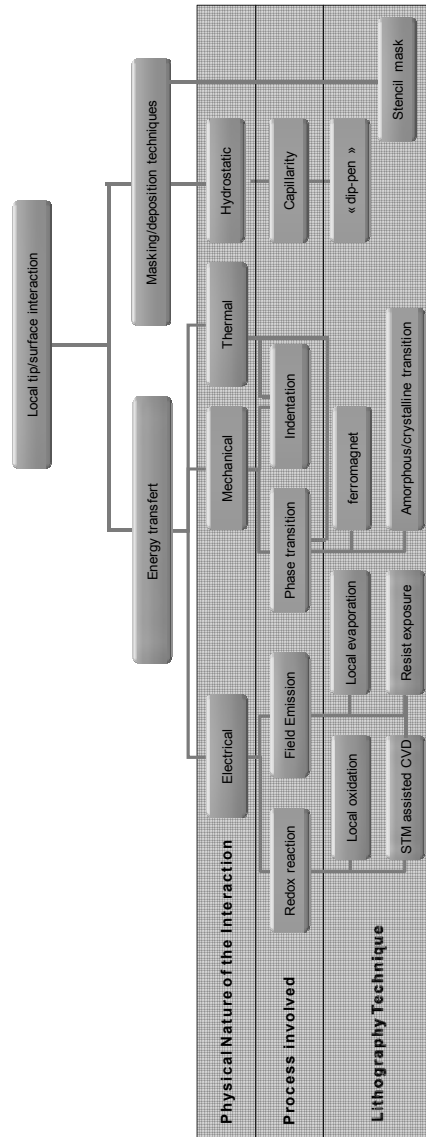


**Figure 3.5.** Classification tree of scanning probe lithography techniques, classified according to the nature of the probe to surface interaction

### 3.4.2. Comparison with competing advanced lithography techniques

Because of their originality, these techniques exhibit features that significantly differ from competing lithographies. Indeed, except in the case of nano-imprint [CHO 95, CHO 98] (described in Chapter 2) and the techniques based on local probes presented in this chapter, it can be seen (Figure 3.5) that the entire group of lithographies (including all those already at an industrial stage) operate at far-field, meaning that the distance between the patterning source and the patterned object is great compared to the size of the patterns obtained. A “far-field” emission requires focalization optical elements combined with high energy radiations (UV photons, X-rays, ions, electrons) [TOR 03]. Optical lithographies (see Chapter 1) and electron beam lithography (Chapter 2) must face diffusion limits and diffractions inherent to this far-field radiation. Their optimization imposes significant technical efforts in order to improve beam emission quality (electron gun, extreme UV sources, etc.) as well as to optimize the beam pathways (such as photonic or electronic lenses and phase shift engineering tools). These efforts have also led to extremely expensive tools.

By contrast, all local-probe microscopes operate only in near field and are not limited by difficulties of this kind. The absence of beam optics provides them with a high potential for reaching ultimate resolutions as well as limiting their integration costs. Furthermore, the resolution limits are those imposed by technology-and not by physics (such as diffraction or diffusion effects). In addition, the possible miniaturization of the writing devices make the tool much more affordable compared to the other techniques. It also has many interesting marketing prospects on a large scale, notably due to a good potential for upscaling and parallelization (for an application example involving information storage, see Figure 3.8 below).

The profound dichotomy between “near-field ” (involving local interaction) and “far-field” (involving beam optics) makes it possible to classify all techniques not according to the nature of the interactions between radiation and matter but according to the distance between the source and the surface (and the presence or not of optical elements).

It is also important to notice that the near-field lithographies (Figure 3.6, right) imply a comparatively smaller energy per pixel. By being “softer”, their resolution is less prone to “proximity effects” [CHA 75]. This effect is linked to the diffusion of incident radiation in the lithographic resist (see the description of basic lithography technologies in Chapter 6). This is an important factor limiting the resolution of far-field lithographies. However, the apparent superiority of the scanning probe techniques does not come without a price to be paid, mainly in terms of throughput.



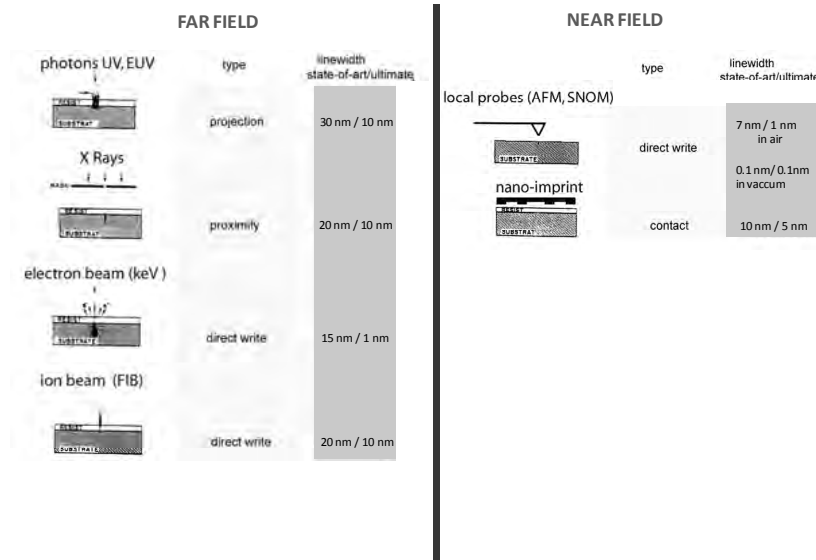


**Figure 3.6.** Comparison of different techniques used to nanostructure surfaces with their associated resolutions. The dichotomy between far-field (left column) and near-field techniques (right column) can be observed

### 3.4.3. Industrial development perspectives

Major disadvantages nowadays limit the application of local-probe lithography techniques on an industrial scale. Two serious disadvantages add up. On one hand they are sequential techniques that require a line to line surface scanning, “in series” (different topolithography or nano-imprint which structure matter in a parallel way). On the other hand, the inertia of the piezoelectric scanning heads considerably limits the moving speed of the tip to a few microns per second, which ranks them as the slowest of lithography techniques (Figure 3.7).

Many recent studies [PIC 07] based on the miniaturization of the piezoelectric heads tend to show that effective scanning speeds are expected to improve a lot in the near future. They would allow the acquisition (and the lithography) using scanning probes at a rate higher than that of video images (25 images per sec.). In addition, the technological pressure coming from disciplines related to nanolithography, such as information storage [MAM 95], is an important motivation to improve microscope technology, mainly by placing the lithography tips in parallel [MIN 98].

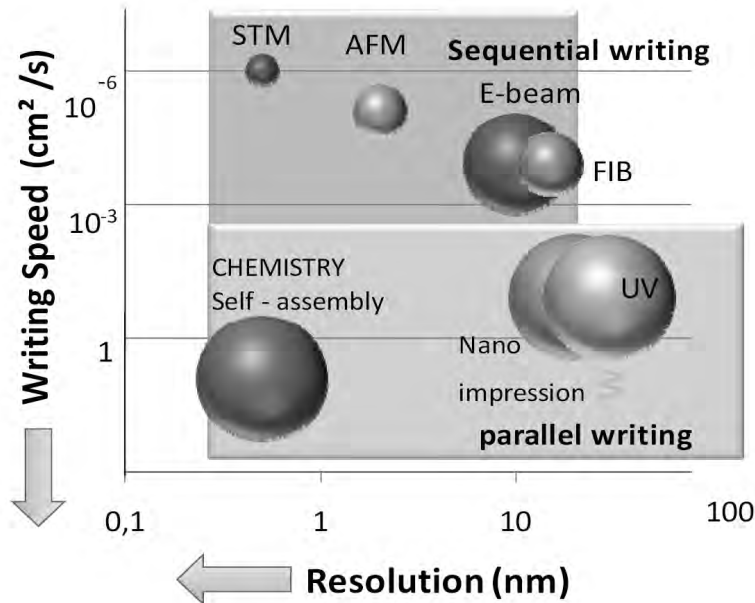


**Figure 3.7.** Graph summarizing all the fabrication techniques including those methods said to be top-down or bottom-up. Methods are classified according to their resolution (X-axis), their writing speed (Y-axis) and their sequential or parallel assembling principle. The near-field techniques appear to be the most precise ones but also the slowest. The parallelization of AFM techniques (represented by a descendant arrow) compensates for their lack of speed

The development of tip rows at Stanford University in 1997, and then of tip arrays at IBM-Zürich (Figure 3.8, left), are improvements that add up to compensate for the lack of speed by means of parallelization. Each tip scans a specific sector. Sophisticated electronic multiplexing allows each tip to be independently addressed and an independent pattern to be created (Figure 3.8, right). It is then possible to reach cumulative scanning speeds in the  $\text{cm}^2/\text{s}$  range. This could therefore turn them into competing techniques compared to electron-beam lithography.

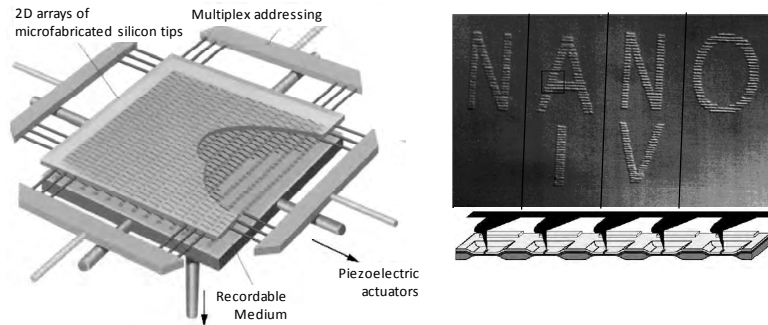


**Figure 3.8.** Left: Fabrication principle of memory of very high density, using a 2D array of tips, each of them scanning a given sector. Writing is achieved using thermo-mechanical indentation on a polymer resist layer, while reading is done by thermoelectric measurements; storage density has been shown to exceed 100Gbit/in<sup>2</sup> (IBM). Right: lithography technique principle using bars of AFM tips. Each tip is addressed by an independent voltage and achieves patterns by scanning a given sector. (Quate group, Stanford University)

### 3.5. Lithographic techniques with polymer resist mask

Further than just demonstrating a controlled way of writing at the nanometric scale, a lithography technique must be introduced into the complete fabrication process, that is to say, it needs to achieve its integration in relation with connectivity and lead to a functional electric prototype. One method to reassure oneself about a technique's compatibility with standard processes of microelectronics is to adapt some process steps (usually the writing step of a mask) while keeping the other steps unchanged (resist deposition, development, mask deposition). One example of this adaptability is the achievement of patterns using electron deposition in a polymer resist. This technique, described in the following section, is usually confined to lithography using scanning electron microscopy.

#### 3.5.1. Electron beam exposure of resists by scanning probe microscopes

Because of the small curvature radius of a sharp tip, it is well-known that field emission occurs for tension of extraction much lower (usually a few tens of volts) than for a planar electrode (more than kV). It is easy to use an atomic force microscope's tip as a low energy electron source. The Calvin Quate group at Stanford University (USA) has conceived a hybrid AFM/STM microscope (see Figure 3.9) including two feedback control loops that allow an independent control of the interaction force and of the electron emission current due to the field-effect.

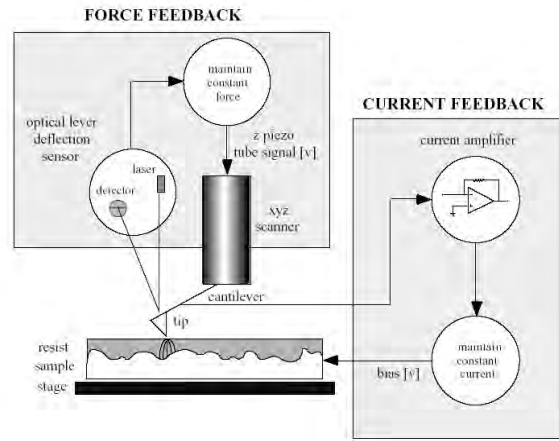


**Figure 3.9.** A local-probe “Hybrid AFM/STM” microscope modified to allow near-field insulation of an electron-sensitive resist. The system includes two independently controlled regulation loops. The force regulation makes it possible to monitor the surface in the same way as for a standard AFM microscope, whereas the regulation of the emission current of the tip allows a given electron quantity per surface unit to be deposited. The emission current of the tip can be controlled in the range ( $1\text{ pA} - 1\text{ nA}$ ) which corresponds to tip tensions around  $40\text{--}60\text{ V}$ . (Figure inspired by [WIL 97])

When a tension is applied to a tip coated with a thin metallic layer making it completely conducting, an electron can be emitted towards the substrate by field emission. The resist layer on the substrate is exposed by the emission current and becomes locally soluble in a developer in a similar way as is done for electron beam lithography (EBL). It is important to notice that the energy of the electrons emitted by the tip (a few tens of electron volts) is much lower than that used in standard e-beam lithography techniques (from  $30$  to more than  $100\text{ kV}$ ). Nonetheless, it is necessary to deposit a much greater quantity of electrons per surface unit. In order to obtain the same resist development, this amount can usually be  $30$  times higher. This looks like an inconvenience because it imposes a physical limit to the scanning speed. However, as already noted, the low electron energy limits their diffusion in the resist and cancels the proximity effect, thus ensuring a perfect linearity of the size and geometry of the lithographed patterns (see Figure 3.10).

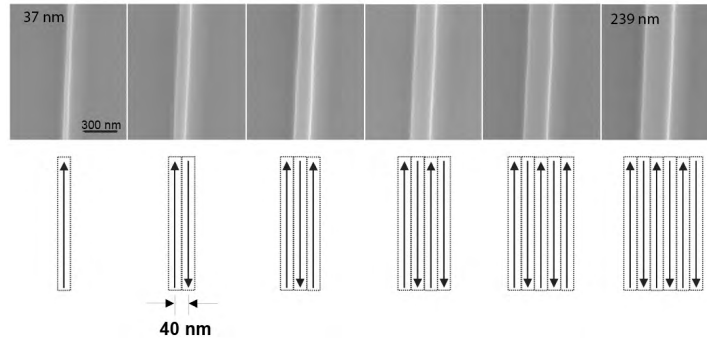


**Figure 3.10.** Micrographies showing lithographed lines after resist development obtained by electronic insulation with an atomic force microscope with its current-polarized tip. The linear dose is 20 nC/cm. The electron energy is 20 eV. The resist profiles of the adjacent lines (40 nm apart) show the perfect linearity of the profile obtained thanks to the number of crossovers and consequently the total absence of proximity effect.

© Quate Group, published in [WIL 98]

### 3.5.2. Development of a resist dedicated to AFM nanolithography

Recent researches have shown that one of the ways to take advantage of local-probe techniques is to develop lithographic resists dedicated to this method instead of using the resists developed for far-field lithography. During the writing process assisted by an electric field, a tension of a few volts between the tip and the surface induces an electric field that can exceed  $10^9$  V/m. Such an intense field decomposes the organic molecules into very reactive fragments which, in addition, induce reactions with the surrounding molecules in a way similar to chemically amplified resists.

For several years now, Jean Fréchet's group at Berkeley University has been developing new lithographic processes based on resists adapted to the specificities of local-probe lithography. Among the significant results, one can note the achievement of a fluorocarbon-based resist with which it is possible to form lithographic patterns 25 nm wide, traced with rates up to 1 cm/s [ROL 07]. Other resists, based on dendrimer compounds have also been developed [ROL 04]. Additional resists containing precursors enabling directed assembly of nano-objects for a nano-structure (for example, lines on which gold nanocrystals will be assembled [GER 08], Figure 3.11) have also been developed.

Another strategy consists of preparing molecules with a chemical bond more sensitive to the electric field, meaning a weak link. Under exposure from the AFM tip, the molecule will always break at this bond [SUE 03].

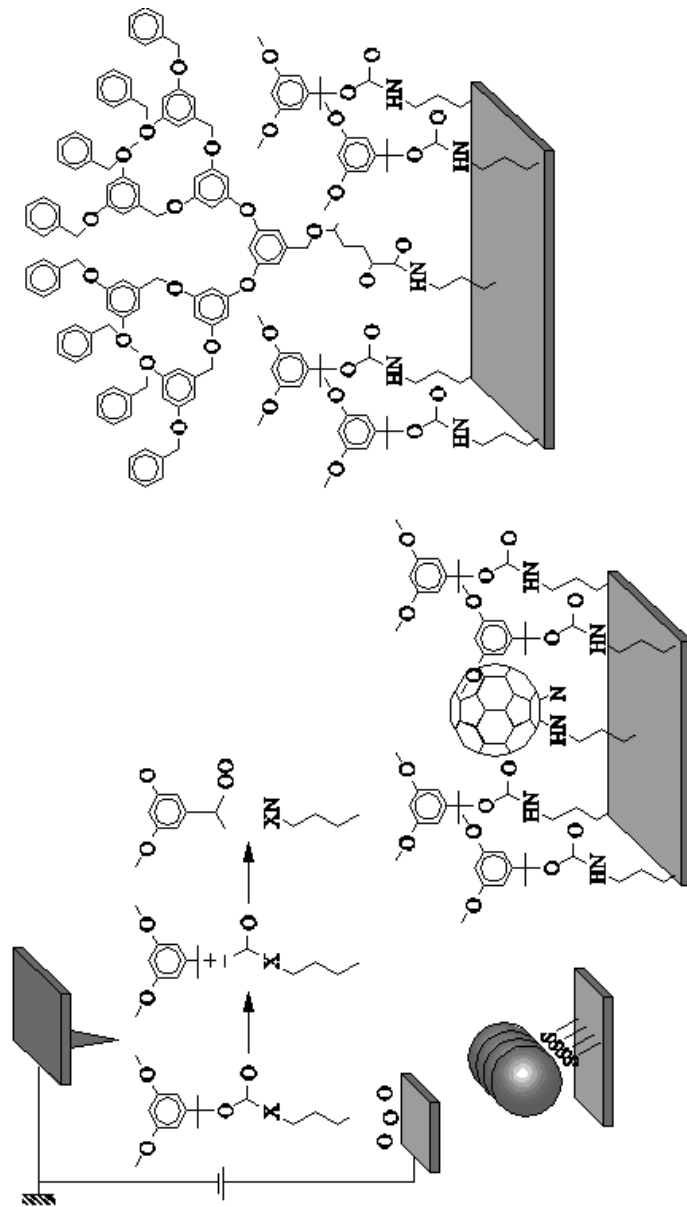


**Figure 3.11.** Use principle of lithographic resist dedicated to local-probe microscopy: depending on the process used, it will allow localized deposition of defined nano-objects such as dendritic macromolecules, metallic nanoparticles or fullerenes. (© Jean Frechet group, U.C. Berkeley)

### 3.5.3. Lithography using mechanical indentation

Another example of mask fabrication consists of using the mechanical properties of the atomic force microscope's tip in order to structure a resist [BOU 96, SOH 95]. Indeed, the sharp profile of AFM tips is well adapted to the achievement of trenches using mechanical indentation. In the image mode, this effect is usually avoided by limiting the interaction force in the nanonewton range. An increase of the control set point of the tip allows much greater interaction forces to be locally induced. The interaction force necessary to obtain indentation is generally in the range of a micronewton. Therefore, it reaches 100 to 1000 times the usual interaction value during imaging. This is equivalent to pressures under the tip in the range of gigapascals, thus being beyond the plastic limit of the polymeric layer for this range of size. In the example we describe, a trench of controlled position and size is achieved using mechanical indentation with an atomic force microscope's tip on a flexible resist. The viscosity of the resist used in this example has been first optimized for this technique (Figure 3.12). The pattern obtained is then transferred into a thin film of germanium by means of plasma etching. The trenches lead to slits which then form a mask after evaporation of the metal under vacuum (Figure 3.13).

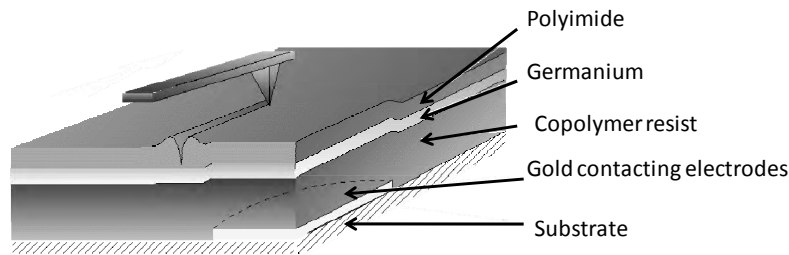


**Figure 3.12.** Schematic of the principle describing the indentation technique of a polyimide resist by means of an atomic force microscope's tip

In association with the oblique angle evaporation technique [DOL 88, ROM 88], it has been shown that this lithography allows one to obtain a functional nanodevice [BOU 96]. A single electron transistor operating at low temperature, with a line width of about 50 nm has been demonstrated. The resolution increase has helped to miniaturize the surface of tunnel junctions, thus improving the charge energy of the transistor island to a single electron and, as a result, its operating temperature. Similarly, mechanical interaction processes of the tip can also be used to modify the nanostructure of an existing device *in situ*. An AFM tip can indeed achieve local erosion on a great number of materials, including metallic thin films [IRM 98], gallium arsenide semi-conducting layers [REG 02], or even monomolecular auto-

assembled layers [WAD 01]. This has enabled the achievement of tridimensional structuring, useful for quantum nanoelectronics, in a way somewhat similar to that obtained by the interaction of a focused ion beam on a surface.

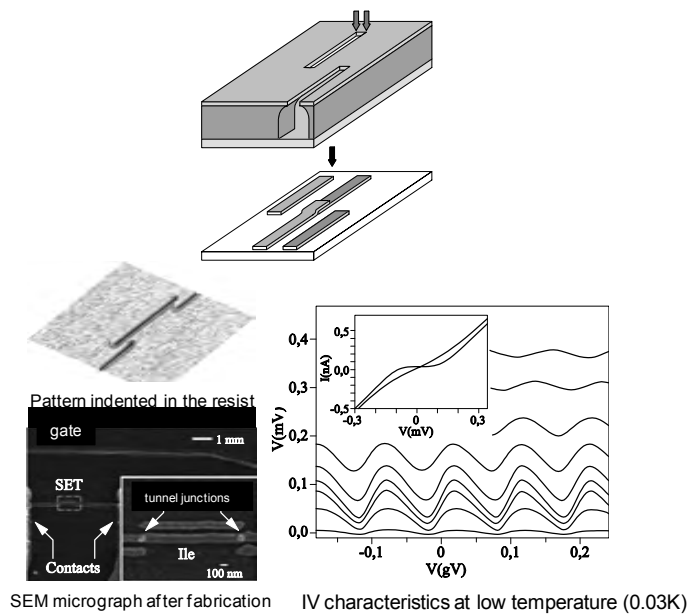


**Figure 3.13.** Oblique angle evaporation principle through a free standing mask (adapted from [BOU 96]), thus allowing the fabrication of a tunnel junction made of aluminum oxide. The partial oxidation of the first layer is achieved before deposition of the second

### 3.6. Lithography techniques using oxidation-reduction interactions

This is the family of local-probe lithography techniques that has led to the greatest number of technical developments and applications.

The principle is simple: it consists of inducing an oxidation-reduction reaction under the microscope's tip when it becomes electrically conducting, and is polarized above a given threshold. The reduced space between the tip and the sample becomes in some sense an electrochemical reactor locally inducing a deposition or modification of the material at the surface. A few examples achieved are given in the following sections.



### 3.6.1. Direct fabrication by means of matter deposition induced by STM microscopy

#### 3.6.1.1. Hydrogenated silicon depassivation by STM

Hydrogenation is a chemical treatment that allows the very reactive dangling bonds that exist at the surface of depassivated single-crystal silicon (in which the native oxide has been stripped) to be neutralized. This hydrogenation consists of replacing them by Si-H bonds which are metastable and allow the surface to be to “passivated” with regards to oxidation. Application of a voltage on a local-probe microscope’s tip (AFM or STM) makes it possible to break the Si-H bond and therefore locally depassivate the surface, thus revealing the dangling bonds once again. The patterned area will then be able to react with a contaminant present in the reactive chamber. This technique’s advantage is the fact that it is generic and that it could be applied to different processes (see, for example, section 3.6.2.1). In addition, it is compatible with a step performed under an ultrahigh vacuum, thus allowing lithographic structures at the scale of a few atoms (Figure 3.14).

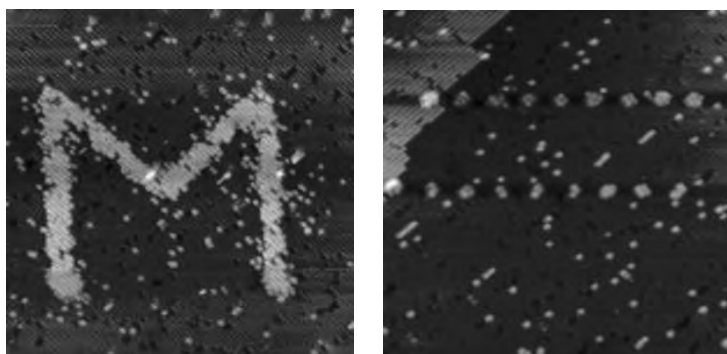


**Figure 3.14.** Micrographs showing lithographic achievements by means of depassivation with an STM microscope on a hydrogenated silicon surface. Left: the letter “M” obtained has a width of approximately 23 nm, with a line width of around 3 nm. Each point on the image corresponds to a depassivated silicon atom. The presence here and there of isolated metastable atoms of hydrogenated silicon can be seen. Right: rows of dots of approximately 15-20 Angstroms in size created by voltage pulses on the tip.  
(Taken from IEMN Lille, adapted from [SYR 99])

#### 3.6.1.2. Local chemical vapor deposition under STM

The controlled local deposition of metallic particles by means of decomposition of a chemical vapor [THI 94] from organometallic compounds (Figure 3.15) is a technique that looks very much like chemical vapor deposition (CVD). Here, the

decomposition of the precursor gas is achieved under the action of an intense electric field that is established between the tip and the sample. This type of deposition is also achievable under a focused beam of gallium ions (FIB) (see Chapter 4). This technique coupled to STM has the advantage of having a nanometric precision specific to local-probe techniques. This process can be precisely controlled in position [MAR 00 ] (Figure 3.15) or, according to the desired volume of deposited material, and enables the simultaneous imaging of the object being lithographed. Moreover, it can be generalized to many different materials, including metals stable in air for nanometric volumes, such as rhodium, for example.

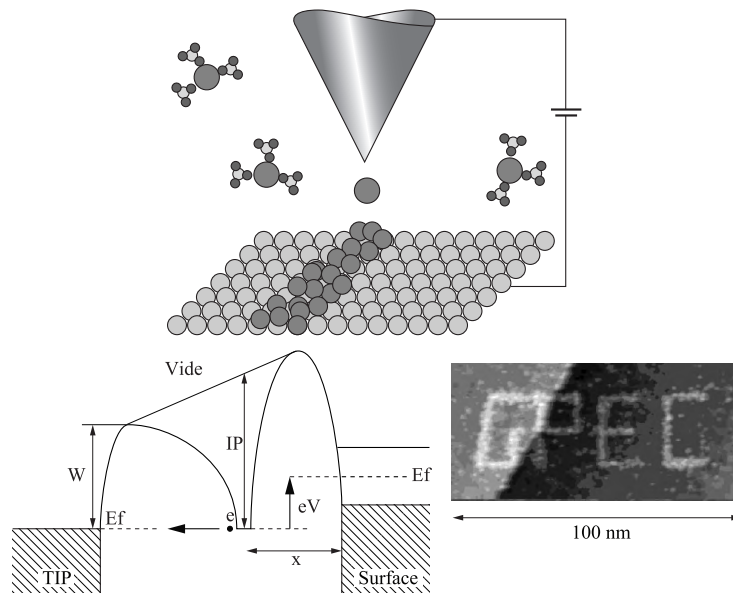


**Figure 3.15.** Top: drawing showing the controlled deposition of a metal from the decomposition of an organo-metallic vapor under the tip of an STM (author's drawing). Bottom, left: energy band diagram showing the decomposition principle by means of the metallic precursor's reduction under the action of a tip-surface electric field and tunnel barriers existing between the tip and the surface (extract from [THI 94]). Bottom, right: ???

The unsolved problem of this technique is the incompatibility that lies in the integration of the particles deposited with the measurement electrodes [MAR 00 ]. It is a recurrent problem of all the advanced nanofabrication techniques but, in this case, there is an additional difficulty which lies in the impossibility of an STM tip to image an electrically insulating area. The use of a hybrid ATM/STM device

of the tip's position is obtained with force interaction, seems therefore essential, if [KAT 97] similar to the one presented in section 3.5.1 and for which the regulation this type of technique is to be pursued further [AMP 05], rather than just being limited to a prototype.

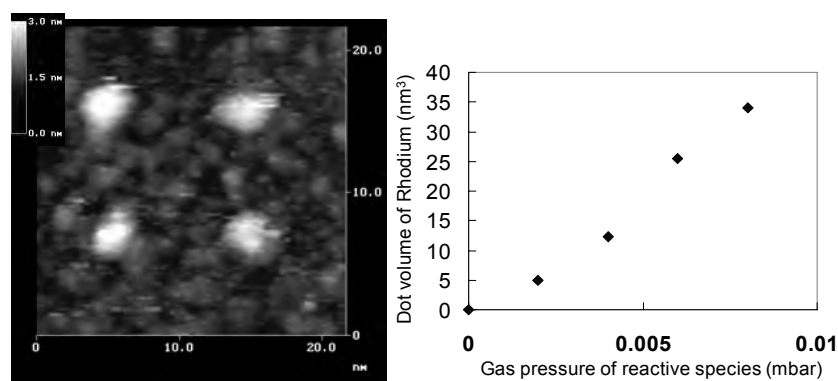


**Figure 3.16.** Left: STM image of an ordered deposition of rhodium nanoparticles corresponding to 3 nm dots. Right: demonstration of the volume control for deposited particles versus precursor gas pressure (taken from [MAR 00]).

### 3.6.2. Local anodization under the AFM tip

This technique is based on surface oxidation, intensified under the atomic force microscope's tip. The anodic oxidation, more widely known as "anodization", concerns an entire family of very diverse processes, of common use in industry, aiming at protecting metals from oxidation. The main idea consists of growing an oxide layer by electrochemical means, such that it becomes impermeable and stable for the material's future use. The local oxidation is in some way the miniaturization of the process in a reactive area between the AFM tip and the surface (Figure 3.17). Unlike previous techniques that require the microscope to be used in a controlled atmosphere, the present process can be used under ambient conditions. Indeed, the water contamination layer existing at the surface of the material leads to the formation of a stable meniscus that will play the role of an electrolyte, the tip being the cathode and the surface, the anode. The high electric field's gradient present in this gap will allow the localization of the reaction over an area of radius less than 10 nm. The mechanism intervening at this scale, described in [STI 97] is two-fold: on one hand, the field induces hydrolysis within the water meniscus leading to reactive ionic species and, on the other hand, it produces a diffusion of the charged oxidizing species below the silicon surface.

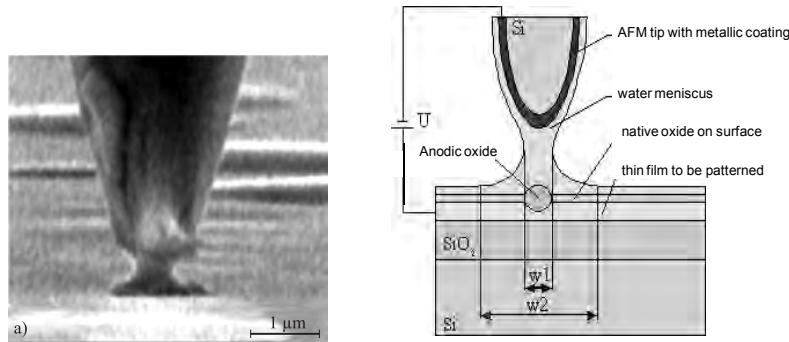


**Figure 3.17.** Left: Micrograph (taken by an environmental electron microscope) showing the existence of the water meniscus at the junction between the tip and the surface, which implements a miniaturized electrochemical medium, from [SCH 98]. Right: Principles of anodization under the atomic force microscope. Due to the potential threshold above which the reaction is activated, the pattern of anodic oxide has a width  $w_1$ , which is of the order of the tip curvature and is below the diameter of the water meniscus  $w_2$

The anodization technique induced by AFM was initially developed on an hydrogenated silicon substrate by J. Dagata (NIST, USA) in 1990 [DAG 90]. He was able to show that it was possible to grow, in a controlled manner, an oxide layer under the voltage biased tip of an AFM. Above a certain voltage threshold from which the oxidation reaction starts, a layer of oxide a few nanometers thick and about 10 nm wide appears under the tip. The oxide quantity (in particular its thickness) can be precisely controlled by the tension applied to the tip as well as the speed rate of the tip. Figure 3.18 shows the precise control of the thickness of a lithographed line of a thin layer of niobium. Many different methods based on the permanent or intermittent contact of the tip as well as on an alternating tension in order to neutralize the space charge effects were subsequently developed.

This process has many advantages compared to other nanolithographic techniques: it is relatively inexpensive and easy to tune. It enables good dimensional control and a precise alignment because the tip – with no applied tension – allows the vicinity of the nanostructure to be visualized in a non invasive way, in turn enabling easy alignment with respect to contacting electrodes. Finally, it allows *in-situ* measurements during the lithography [SNO 95], allowing one to stop the process at an exact moment [SNO 96] no longer depending on the geometry but on the required electrical properties (device resistance, for example). This process can be applied on either silicon or ultra-thin metallic films and makes it possible to process quantum devices [SNO 96].

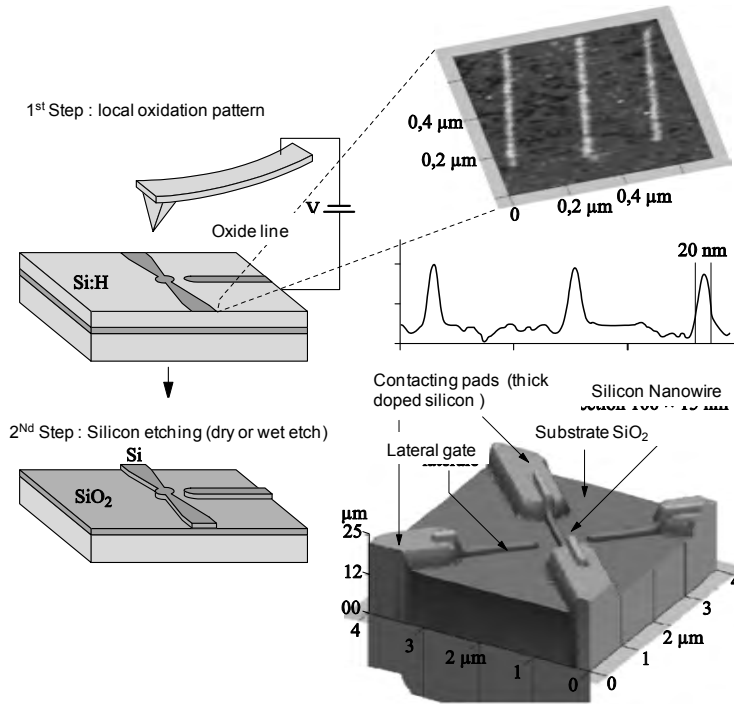


**Figure 3.18.** Left: schematic of the fabrication process principle for silicon nanostructures by means of AFM nano-oxidation. The first step consists of the anodization by AFM of a silicon layer on an insulator previously hydrogenated on its surface. The local oxidation creates a contrast of a chemical nature between silicon and silicon oxide (height  $\sim 1$  nm) which is developed during the wet etching of the silicon not protected by the oxide. This results in connected single-crystal nanostructures, on oxide

The fabrication of an oxide line on a hydrogenated silicon substrate (the substrate is similar to the one described in 3.6.1.1.) therefore enables silicon oxide lines to be achieved in precise spots on the sample. The key point consists of taking advantage of these oxide nanostructures by a process involving ultra-thin layers of a conducting material.

#### 3.6.2.1. Application to the fabrication of silicon nanostructures

The first process described in this section concerns the application of AFM nano-oxidation to achieve nanostructures on thin layers of silicon-on-insulator [SNO 95]. Such a lithographed oxide wire behaves like a mask (Figure 3.18) capable of

protecting the underlying material against a silicon attack by wet etching [TAB 92]. Therefore, the oxide wire protects the non-oxidized underlying material in a very efficient way (usually a fraction of a nanometer is enough to protect 20 nm of underlying silicon) and allows a structure in the silicon film to be freed (see Figure 3.18). This technique is completely adapted to the achievement of silicon-on-insulator (SOI) nanostructures [SNO 94]. The advantage of using SOI materials comes from the fact that the protected silicon is supported by an insulator substrate of buried oxide and allows electronic nanostructures supported on oxide to be produced (see Figure 3.18). The first studied structures were single-crystal silicon channels of connected nanometric diameter [CAM 95]. A lateral “finger” approaching this nanowire can be used as the gate and allows the fabrication of a field effect transistor for which the interaction between the electric field of the gate and the channel can be confined to distances of up to a few dozen nanometers (Figure 3.19). Such a device shows interesting electronic properties, more precisely for low temperatures where it can implement single electron devices [CLE 02].

This technique, which could in principle be included in a “standard” microelectronic process (implying other “standard” lithography processes like masking and etching) [BOU 02], offers a great flexibility towards the geometry of required structures (Figure 3.20). It is important to notice the low roughness of the nanostructures obtained (compared to similar structures obtained by means of plasma etching) since all the processes are achieved in a liquid phase. Very recent results show that it is possible to push this technology up to achieving functional transistors of a channel width of about 4 nm [MAR 08]. This nano-oxidation process coupled to silicon-on-insulator also allows the fabrication of free standing electromechanical devices of very high resolution [VIL 04].

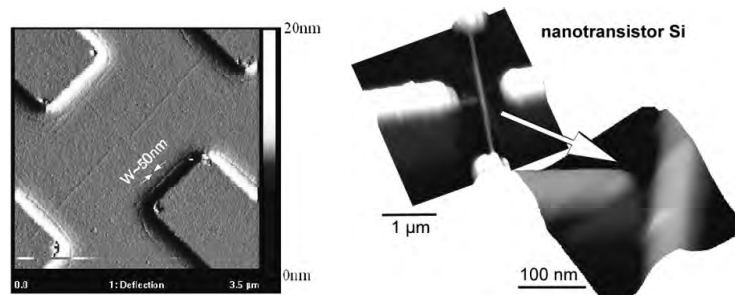


**Figure 3.19.** Left: oxide lines before etching for the fabrication of a lateral gate transistor. Although their thickness is around 1 nm, the etching selectivity allows a reliable etching mask to be achieved. Right: device after the etching step, a simple silicon channel of diameter  $50 \times 15 \text{ (nm)}^2$

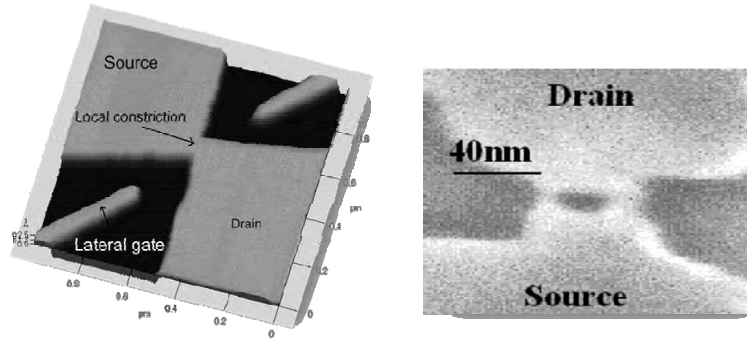


**Figure 3.20.** Left: AFM micrograph of silicon local constriction addressed by side gates. Right: MEB micrograph of a nanostructure with two parallel channels; the width of the channels is around 15 nm. Notice the regularity and the weak roughness of the etched surfaces, characteristic of silicon wet etching [TAB 92]

#### 3.6.2.2. Application to ultra-thin metallic film oxidation

This oxidation technique is also very well adapted to superconducting and metallic layers. These layers of a thickness of a few nanometers (usually 3 to 10 nm) are thin enough to induce metal oxidation under the tip in the whole thickness, from which a controlled electrical separation [SNO 95] between the parts located on each side of the oxide line results (Figure 3.21). Nanostructures of relative complex shape can be made by limiting their shape and defining boundaries by AFM drawn insulating oxide lines (Figure 3.22), since the purpose of the lines is to limit or even interrupt the electronic conduction.

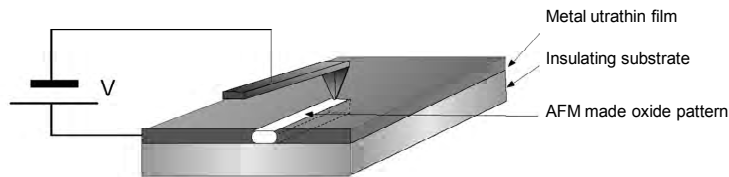


**Figure 3.21.** Principle of local oxidation in AFM applied to ultra-thin metallic films. Unlike the nanooxidation on silicon described in the previous sections, for which the lithographic area corresponds to the conducting part after etching, this second process presents a “negative” direct writing where the insulating oxide pattern locally neutralizes the metal layer. The resolution obtained enables accurate control of the final metallic structure shape, in the range of 15 nm

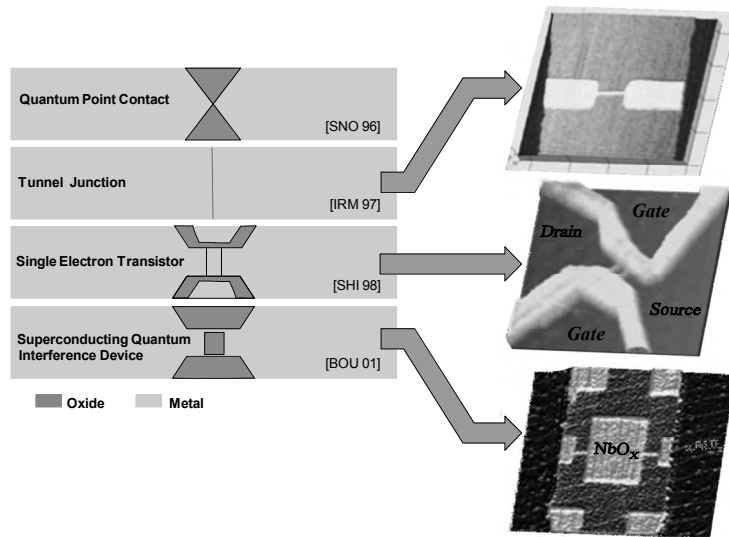


**Figure 3.22.** Left: Diagrams presenting different functional quantum devices achieved by AFM lithography on metallic ultra-thin layers. The AFM patterned insulating areas are in gray. The thinner lines are semi-transparent barriers that let the current through and implement in-trench tunnel barriers. Right: AFM micrographies of standard samples

The dimensional control of a semi-conductor quantum dot obtained by lithography based on these techniques of nano-oxidation was demonstrated by the ENSSLIN team at ETH Zürich in 1997 [HEL 97]. The process is based on the nano-oxidation of an ultra-thin film of titanium which produces submicron local gates on a 2D electron gas. Next, it was shown by the same team [HEL 98], that the titanium film could be removed and that the oxidation could be induced in the heterostructure. This technique proved to be successful by revealing new interference processes in quantum rings [FUH 01] obtained by lithographic techniques.

At the same time, semi-conducting heterostructures were studied. Matsumoto's team in Japan (Electrotech Lab, Tsukuba) focused on the nanostructuring of titanium and niobium ultra-thin films [MAT 96]. In 1998, they demonstrated a single-electron transistor operating at ambient temperature [SHI 98]. The success of this technique is the result of mastering a lithography allowing metals to be structured at a sub-50 nm scale, combined with the realization of ultra-thin niobium layers (less than 10 nm thick) which have specific electrical characteristics.



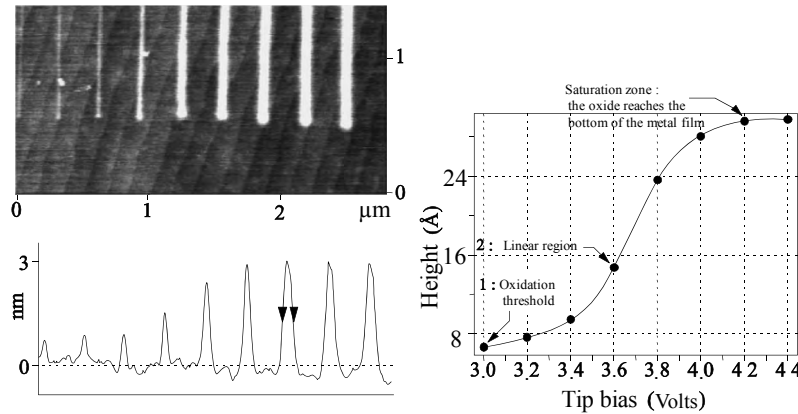


**Figure 3.23.** Series of oxide lines patterned on an epitaxial niobium layer grown on a sapphire substrate for increasing tip tensions. The 3 anodic oxidation regimes used, under AFM for an ultra-thin layer, were: 1. oxidation threshold (here 3 V); 2. linear regime; 3. Saturation regime for which the entire layer was oxidized, pushing the oxide towards the side and increasing the line width

Single-electron electronic developments [GRA 92] over the last 20 years and, more recently, superconducting technologies applied to quantum information (Superconducting Qubits) rely almost entirely on a unique technology, that is to say the aluminum/aluminum oxide-type tunnel junctions obtained by electron beam lithography, and then oblique angle evaporation through a free standing mask (Figure 3.13, left).

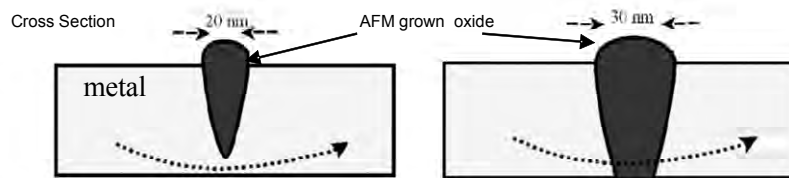


**Figure 3.24.** Cross sections perpendicular to an AFM grown oxide single pixel line (image adapted from [IRM 97]). Left: Incomplete oxidation in the thickness showing a variable thickness constriction leading to a remaining metallic neck around the substrate. Right: complete oxidation realized at higher tip bias, realizing an in-trench tunnel junction

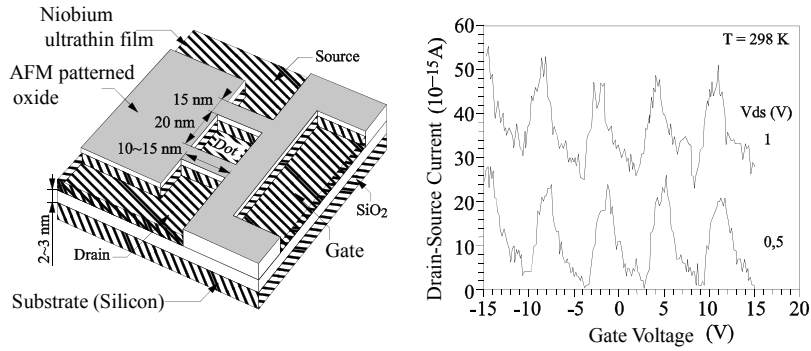


**Figure 3.25.** Fabrication, by means of oxidation under AFM, of the first single electron transistor (SET) operating at ambient temperature. Left: Structure schematics, the light grey areas are the insulating parts achieved by AFM. Right: drain-source current oscillations as a function of gate tension. Each period corresponds to a polarized electron at the gate. (Figure adapted from K. Matsumoto, ETL, Tsukuba, Japan 1997)

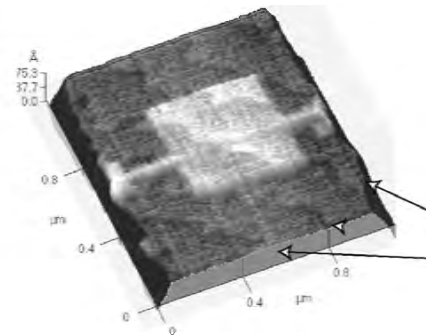


**Figure 3.26.** Interferometer device achieved by means of AFM oxidation of a niobium layer. The light colored surfaces correspond to the areas oxidized by AFM scanning. The arrows show the replication of the atomic steps of the sapphire at the surface. They are also present at the surface of the anodic oxide traced by AFM (central surface, light colored). The atomic step height is equal to the distance between to niobium atoms, meaning 0.3 nm. The precise control of the oxidation quantity is a guarantee of the quality and of the reproducibility of the nanostructures obtained

With the help of these new anodic oxidation techniques, original techniques have been elaborated to try to make them free from successive evaporations. By precisely controlling the oxidation parameters of the AFM tip, it is possible to reduce the

width of the oxide barrier up to the point where it allows a tunnel coupling to be established between the two lateral electrodes. However, the oxide nature and the homogeneity of its thickness are decisive for the tunnel barrier quality [IRM 97]. This tends to prove that the tunnel transport mainly takes place through the defects of the oxide barriers (pin-holes). Additional applications of these techniques have been obtained by the observation of superconductivity properties of the lithographed objects [BOU 01].

By optimizing the lithography parameters to only oxidize part of the thickness of these films, it is possible to reduce the diameter of the superconducting nanowires. This is illustrated by the fabrication of a miniaturized superconducting quantum interferometer (Figure 3.26) for which the size of the active elements allows the magnetometric detection of nanometric magnets to be considered.

### 3.6.2.3. Advantage of tips grafted by carbon nanotubes

AFM tips with carbon nanotubes at their end have been rapidly used in order to improve the performances of local-probe anodization techniques [DAI 98]. Nanotubes were already known [DAI 96] for their remarkable properties for AFM imaging when grafted on a tip's end: their high rigidity compared to their size, as well as their small diameter allows the resolution and stability of the acquired images in the intermittent contact mode to be improved in a noticeable way.

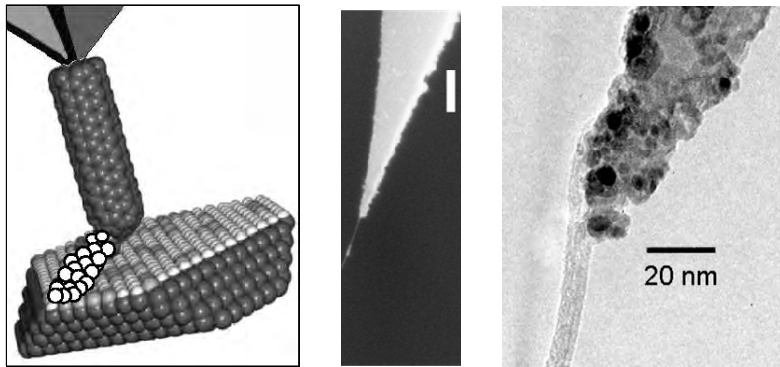


**Figure 3.27.** Left: principle schematic showing oxide growth at the end of an AFM tip grafted by a carbon nanotube. The hydrophobicity of the nanotube considerably reduces the extension of the water meniscus. Center and right: electronic micrographs (center: scanning microscopy, right: transmission microscopy) showing controlled grafting obtained by in situ growth of a carbon nanotube by a chemical vapor deposition technique [MAR 06]

Furthermore, there are two additional interesting properties when these tips are used for AFM nano-oxidation: on one hand, the electric field is focused by the nanotube and on the other hand, the hydrophobic characteristic of the nanotube surface [KUR 07] reduces the lateral extension of the water meniscus (Figure 3.28). These two effects contribute to improve the stability of the lithography as well as the lateral resolution of the obtained oxide lines for which the current record is 7 nm [COO 99]. In addition, the remarkable mechanical properties of nanotubes enable very high writing speeds of around 100  $\mu\text{m/s}$  while keeping good tip durability.

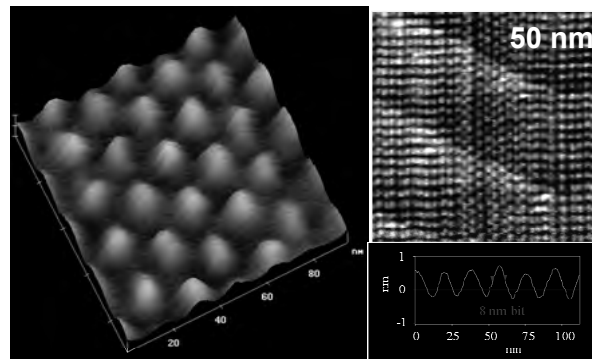


**Figure 3.28.** Demonstration of anodization of a niobium layer by means of a nanotube grafted tip. The AFM micrograph shows that the point density obtained by this technique is 15 terabytes/ inch<sup>2</sup>. Adapted from [COO 99]

### 3.7. “Passive” lithography techniques

This sub-family of near-field lithography techniques groups together the most recent lithography techniques for which the tip does not behave as a local energy source (thus the name of passive techniques). The localization possibilities of the tip are used to achieve a precise alignment on the surface and produce a local deposition by means of capillarity (dip-pen lithography) or of masking (stencil mask).

#### 3.7.1. Dip-pen lithography

In 1998, a team directed by Chad Mirkin at Northwestern University, Illinois, elaborated a new technique called dip-pen lithography for which the microscope’s tip is coated beforehand with a liquid that is able to deliver, at a given point, a controlled quantity of matter. This technique makes the most out of the capillarity

forces that successively collect a small liquid quantity from the tip's surface to release it in a controlled way.

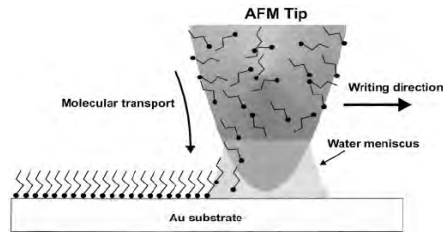


**Figure 3.29.** Principle of Dip-pen lithography

The principle of dip-pen lithography is very similar to the dipping of a pen into an inkwell. The tip is coated beforehand with a small quantity of liquid by soaking it in a humid zone (the inkwell) which wets the tip's surface by capillarity. The tip is then moved and put in contact with the surface according to a predetermined pattern of points. The time during which the tip remains on a specific surface precisely determines the liquid quantity deposited at each point. Diffusion principles show that the size increase of the deposited objects vary with the square root of the time that the tip stays on the surface. It is important to notice that the controlled deposition of very small quantities (controlled deposition of dip-pen lithography fluids [PIN 99]) has relevant applications for molecular biology [LEE 02].

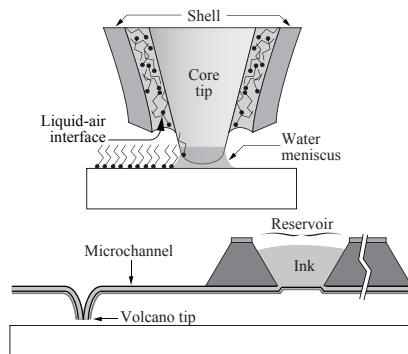


**Figure 3.30.** Schematic cross-section of a second generation dip-pen stylograph's tip, with an ink reservoir, thanks to the integration of a micro-fluidic technology at the tip. This recent improvement makes it possible to remove the backward and forwards movements towards the position of the ink reservoir (no further need for an inkwell) and also improves the deposition speed and precision. © C. Mirkin

### 3.7.2. Alignment technique by means of a mechanical masking (stencil mask)

This technique is the adaptation to local-probe lithography techniques of the possibilities of making material deposition in the presence of mechanical masks (called stencil masks) [DES 99]. The added value here is linked to the alignment properties of the mechanical masks thanks to atomic force microscopy [PER 02]. Unfortunately, these masking techniques with the tip are still not well known. This technique is roughly using the AFM tip as a stencil during the vacuum evaporation of a thin metallic layer, or during ion irradiation of the surface [MEI 06, PER 04]. The shadowing of the tip, correctly positioned in relation to a nanostructure, allows, for example, that nanostructure to be connected to metallic electrodes. The fabrication of dedicated tips (for example with a central channel driven by focused ion beam techniques, Figure 3.31) enables the optimization of the stencil's shape.

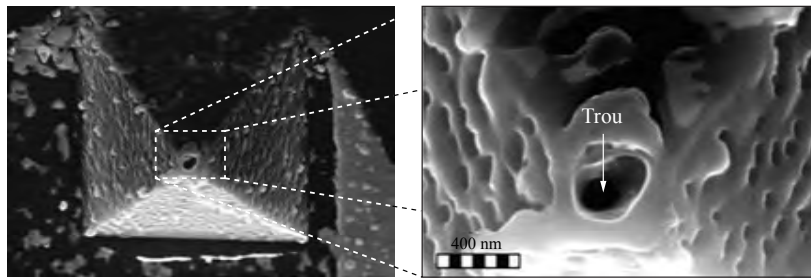


**Figure 3.31.** Micrography by scanning electron microscopy of an AFM silicon nitride tip, the symmetry axis of which has been drilled by a focused ion beam. Such a tip makes it possible to geometrically confine matter deposition by means of shadowing and enables the achievement of lines by moving the tip during deposition. From [MEI 06]

The on-going applications of this technique concern the possibility of delivering doping impurities or even a single dopant at precise points [SCH 06]. If applied to controlled doping of a silicon channel, it is expected to achieve a quantum bit by using the electron spin of the ion impurity [SCH 03] inside the silicon matrix as the quantum information medium. Similar research concerning diamond crystal radiation, useful for quantum information, are in progress [MEI 06].

### 3.8. Conclusions and perspectives

Through the presentation of this brief overview we intend to show the remarkable application potential of local-probe microscopy techniques for nanolithography. Beyond their ultimate resolution (1 to 10 nm, depending on the

process chosen), what must be remembered is the extreme versatility of these techniques, a guarantee of still further innovation.

It is interesting to notice that these techniques are at the convergence of the complementary *top-down* (matter structuring – considered as a homogeneous continuum – by thinner and thinner lines) and *bottom-up* (construction with elementary components: atoms, molecules) approaches. Their relative confidentiality and their low industrial impact are granted by the fact that the tuning of the lithographic parameters remains a traditional and time-consuming task. Unlike the competing techniques based on microscopes developed 50 years ago, local probes are still young and their maturity is far from being reached. They are also financially attractive because of their possible miniaturization, thanks to the developments of embedded electronics. Unfortunately an essential aspect is often forgotten: the obligation of escorting these new lithographic processes by developing bespoke materials (new resists, single-crystal ultra-thin layers) in order to benefit from all the potential of these surface microscopy techniques.

### 3.9. Bibliography

- [ALB 89] ALBRECHT T.R., DOVEK M.M., KIRK M.D., LANG C.A., QUATE C.F., SMITH D.P.E., “Nanometer-Scale Hole Formation on Graphite Using a Scanning Tunneling Microscope”, *Applied Physics Letters*, 55, p. 1727–9, 1989.
- [AMP 05] AMPERE A.T., ANDREA N., CHEN T.P., “Nanofabrication by Scanning Probe Microscope Lithography: A Review”, *Journal of Vacuum Science & Technology B: Microelectronics and Nanometer Structures*, 23, p. 877–894, 2005.
- [AVO 98] AVOURIS P., MARTEL R., HERTEL T., SANDSTROM R., “AFM-Tip-Induced and Current-Induced Local Oxidation of Silicon and Metals”, *Applied Physics A: Materials Science & Processing*, 66, p. S659–S667, 1998.
- [AVO 99] AVOURIS P., HERTEL T., MARTEL R., SCHMIDT T., SHEA H.R., AND WALKUP R.E., “Carbon Nanotubes: Nanomechanics, Manipulation, and Electronic Devices”, *Appl. Surf. Science*, 141, p. 201, 1999.
- [BIN 86] BINNIG G., QUATE C.F., GERBER C., “Atomic Force Microscope”, *Physical Review Letters*, 56, p. 930, 1986.
- [BIN 82] BINNING G., ROHRER H., GERBER C., WEIBEL E., “Surface Studies by Scanning Tunneling Microscopy”, *Physical Review Letters*, 49, p. 57, 1982.
- [BOU 96] BOUCHIAT V., ESTEVE D., “Lift-off lithography using an atomic force microscope”, *Appl. Phys. Lett.*, 69, p. 3098, 1996.

- [BOU 01] BOUCHIAT V., FAUCHER M., THIRION C., WERNSDORFER W., FOURNIER T., PANNETIER B., "Josephson Junctions and Superconducting Interferences devices made by local anodisation of niobium ultra-thin films", *Applied Physics Letters*, vol.79, p. 123, 2001.
- [BOU 02] BOUCHIAT V., FAUCHER M., FOURNIER T., PANNETIER B., THIRION C., WERNSDORFER W., CLÉMENT N., TONNEAU D., DALLAPORTA H., SAFAROV S., VILLEGIER J.C., FRABOULET D., MARIOLLE D., GAUTIER J., "Resist-Less Patterning of Quantum Nanostructures Using an Atomic Force Microscope", *Microelectronic Engineering*, 61–62, p. 517–22, 2002.
- [CAM 95] CAMPBELL P.M., SNOW E.S., McMARR P.J., "Fabrication of nanometer-scale side-gated silicon field effect transistors with an atomic force microscope", *Appl. Phys. Lett.*, vol. 66, p. 1388–90, 1995.
- [CHA 75] CHANG T.H.P., "Proximity Effect", *J. Vac. Sci. Technol.*, 12, p. 1271, 1975.
- [CHO 95] CHOU S.Y., KRAUSS P.R., Renstrom, P.J., "Imprint of sub-25 nm vias and trenches in polymers", *Applied Physics Letters*, vol. 67 p. 3114, 1995.
- [CHO 98] CHOU S.Y., Nanoimprint lithography US Patent 5,772,905, USA, 1998.
- [CLE 02] CLÉMENT N., BOUCHIAT V., TONNEAU D., DALLAPORTA H., FRABOULET D., MARIOLLE D., GAUTIER J. AND SAFAROV V., "Electronic transport properties of single crystal silicon nanowires fabricated using an Atomic Force Microscope", *Physica E: Low-dimensional Systems and Nanostructures*, 13, p. 999–1002, 2002.
- [COO 99] COOPER E.B., MANALIS S.R., FANG H., DAI H., MATSUMOTO K., MINNE S.C., HUNT T., QUATE C.F., "Terabit-Per-Square-Inch Data Storage with the Atomic Force Microscope", *Applied Physics Letters*, 75, p. 3566–8, 1999.
- [CRO 93] CROMMIE M. F., LUTZ C. P., AND EIGLER D. M., "Confinement of Electrons to Quantum Corrals on a Metal Surface", *Science* Vol. 262, p.218 – 220, 1993.
- [DAG 90] DAGATA J.A., SCHNEIR J., HARARY H.H., EVANS C.J., POSTEK M.T., BENNETT J., "Modification of Hydrogen-Passivated Silicon by a Scanning Tunneling Microscope Operating in Air", *Applied Physics Letters*, 56, p. 2001–3, 1990.
- [DAI 98] DAI H., FRANKLIN N., HAN J., "Exploiting the Properties of Carbon Nanotubes for Nanolithography", *Applied Physics Letters*, 73, p. 1508–1510, 1998.
- [DAI 96] DAI H., HAFNER J.H., RINZLER A.G., COLBERT D.T., SMALLEY R.E., "Nanotubes as Nanoprobes in Scanning Probe Microscopy", *Nature*, 384, p. 147–50, 1996.
- [DES 99] DESHMUKH, M., RALPH D.C., THOMAS M., SILCOX J., "Nanofabrication using a stencil mask", *Appl. Phys. Lett.*, 75, 1631 (1999)
- [DOL 88] DOLAN G.J., DUNSMUIR J.H., "Very Small (20 nm) Lithographic Wires, Dots, Rings, and Tunnel Junctions", *Physica*, B 152, p. 7, 1988.
- [EIG 90] EIGLER D.M., SCHWEIZER E.K., "Positioning Single Atoms with a Scanning Tunnelling Microscope", *Nature*, 344, p. 524, 1990.



- [FUH 01] FUHRER A., LÜSCHER S., IHN T., HEINZEL T., ENSSLIN K., WEGSCHEIDER W., BICHLER M., “Energy spectra of quantum rings”, *Nature*, 413, p. 822, 2001.
- [GAR 06] GARCIA R, MARTINEZ RV & MARTINEZ J., “Nano-Chemistry and Scanning Probe Nanolithographies”, *Chem. Soc. Rev.*, 35, p. 29, 2006.
- [GOR 95] GORDON A.E., FAYFIELD R.T., LITFIN D.D., HIGMAN T.K., *AVS*, 2805–8, 1995.
- [GRA 92] GRABERT H., DEVORET M.H. *Single Charge Tunneling Coulomb Blockade Phenomena in Nanostructures*, Plenum Press, New York, 1992.
- [HEI 94] HEINZELMANN H., POHL D.W., “Scanning near-Field Microscopy” *Applied Physics A: Materials Science & Processing*, 59, p. 89, 1994.
- [HEL 97] HELD R., HEINZEL T., STUDERUS P., ENSSLIN K., HOLLAND M., “Semiconductor quantum point contact fabricated by lithography with an atomic force microscope” *Appl. Phys. Lett.*, 71, 2689, 1997.
- [HEL 98] HELD R., VANCURA T., HEINZEL T., ENSSLIN K., HOLLAND M., WEGSCHEIDER W., “In-plane gates and nanostructures fabricated by direct oxidation of semiconductor heterostructures with an atomic force microscope”, *Appl. Phys. Lett.*, 73, 262, 1998.
- [IRM 97] IRMER B., KEHRLE M., LORENZ H., KOTTHAUS J.P., “Fabrication of Ti/TiO<sub>x</sub> Tunneling Barriers by Tapping Mode Atomic Force Microscopy Induced Local Oxidation”, *Applied Physics Letters*, 71, p. 1733–1735, 1997.
- [IRM 98] IRMER B., *et al.*, “Josephson junctions defined by a nanoplough”, *Applied Physics Letters*, 73 (14), p. 2051–2053, 1998.
- [KAT 97] KATHRYN W., HYONGSOK T.S., ABDULLAH A., CALVIN F.Q., “Hybrid Atomic Force/Scanning Tunneling Lithography”, *Journal of Vacuum Science & Technology B: Microelectronics and Nanometer Structures*, 15, p. 1811–7, 1997.
- [JUN 98] JUNNO T., CARLSSON S.-B., XU HONGQI, MONTELIUS L., AND SAMUELSON L., “Fabrication of quantum devices by Ångström-level manipulation of nanoparticles with an atomic force microscope”, *Applied Physics Letters*, 72 (5): p. 548, 1998.
- [KUR 07] KURAMOUCHI H., TOKIZAKI T., YOKOYAMA H., DAGATA J.A., “Why Nano-Oxidation with Carbon Nanotube Probes Is So Stable: I. Linkage between Hydrophobicity and Stability”, *Nanotechnology*, 18, p. 135703, 2007.
- [LEB 97] LEBRETON C., WANG Z.Z., “Nano-hole formation on gold surface using scanning tunnelling microscope”, *Appl. Phys.*, A 66, S777–S782, 1998.
- [LEE 02] LEE K.B., PARK S.J., SMITH C.A.M.C., MRKSICH M., “Protein Nanoarrays Generated by Dip-Pen Nanolithography” *Science*, 295, p. 1702, 2002.
- [LYD 96] LYDING J.W., SHEN T.C., ABELN G.C., WANG C., TUCKER J.R., “Nanoscale patterning and selective chemistry of silicon surfaces by ultrahigh-vacuum scanning tunneling microscopy”, *Nanotechnology*, 7, p. 128–133, 1996.

- [MAM 95] MAMIN H.J., TERRIS B.D., FAN L.S., HOEN S., BARRETT R.C., RUGAR D., "High-density data storage using proximal probe techniques", *IBM Journal of Research and Development*, 39, p. 681, 1995.
- [MAR 00A] MARCHI F., TONNEAU D., DALLAPORTA H., PIERRISNARD R., BOUCHIAT V., SAFAROV V., DOPPELT P., EVEN R., "Nanometer Scale Patterning by Scanning Tunneling Microscope Assisted Chemical Vapour Deposition", *Microelectronic Engineering*, 50, p. 59, 2000.
- [MAR 00B] MARCHI F., TONNEAU D., BOUCHIAT V., DALLAPORTA H., SAFAROV V., DOPPELT P., EVEN R., BEITONE L., "Direct Patterning of Noble Metal Nanostructures with a Scanning Tunneling Microscope", *Journal of Vacuum Science & Technology*, B 18, p. 1171, 2000.
- [MAR 06] MARTY L., IAIA A., FAUCHER M., BOUCHIAT V., NAUD C., CHAUMONT M., FOURNIER T., BONNOT A.M., "Self-assembled single wall carbon nanotube field effect transistors and AFM tips prepared by hot filament assisted CVD", *Thin Solid Films*, 453, p. 1024–1027, 2006.
- [MAR 08] MARTINEZ J., MARTINEZ R.V., GARCIA R., "Silicon Nanowire Transistors with a channel width of 4 nm Fabricated with Atomic Force Nanolithography", *Nano Letter*, vol. 8, p. 3636–39, 2008.
- [MAR 98] MARCHI F., BOUCHIAT V., DALLAPORTA H., SAFAROV V., TONNEAU D., DOPPELT P., "Growth of Silicon Oxide on Hydrogenated Silicon During Lithography with an Atomic Force Microscope", *Journal of Vacuum Science and Technology*, B 16, p. 2952, 1998.
- [MAT 96] MATSUMOTO K., ISHII M., SEGAWA K., OKA Y., VARTANIAN B.J., HARRIS J.S., "Room T Set Par Stm", *Appl. Phys. Lett.*, 68, p. 34, 1996.
- [MEI 06] MEIJER J., *et al.*, "Concept of deterministic single ion doping with sub-nm spatial resolution" *Appl. Phys.*, A, vol. 83, 2006.
- [MIN 98] MINNE S.C., YARALIOGLU G., MANALIS S.R., ADAMS J.D., ZESCH J., ATALAR A., QUATE C.F., "Automated Parallel High-Speed Atomic Force Microscopy", *Appl. Phys. Lett.*, 72, p. 2340, 1998.
- [MOR 00] MORIMOTO K., PEREZ-MURANO F., DAGATA J.A., "Density Variations in Scanned Probe Oxidation" *Applied Surface Science*, 158, p. 205, 2000.
- [PER 04] PERSAUD A., ALLEN F., GICQUEL F., PARK S.J., LIDDLE J.A., SCHENKEL T., IVANOV T., IVANOVA K., RANGELOW I.W., BOKOR J., "Single ion implantation with scanning probe alignment", *J. Vac. Sci. Tech.*, B 22, p. 3115–3118, 2004.
- [PIC 07] PICCO L.M., BOZEC L., ULCINAS A., ENGLEDEW D.J., ANTIGNOZZI M., HORTON M.A., MILES M.J., "Breaking the Speed Limit with Atomic Force Microscopy", *Nanotechnology*, 18, p. 044030, 2007.
- [PIN 99] PINER R.D., ZHU J., XU F., HONG S., MIRKIN C.A., "Dip-Pen Nanolithography", *Science*, 283, p. 661–3, 1999.

- [REG 02] REGUL J., KEYSER U.F., PAESLER M., HOHLS F., ZEITLER U., HAUG R., MALAVE J.A., OESTERSCHULZE E., REUTER D., WIECK A.D., "Fabrication of quantum point contacts by engraving GaAs/AlGaAs heterostructures with a diamond tip", *Appl. Phys. Lett.*, 81, p. 2023, 2002.
- [ROL 04] ROLANDI M., SUEZ I., DA, H., FRÉCHET J.M.J., "Dendrimer Monolayers as Negative and Positive Tone Resists for Scanning Probe Lithography", *Nanolett.*, 4, 889–893, 2004.
- [ROL 07] ROLANDI M., SUEZ I., SCHOLL A., FRÉCHET J.M.J., "Fluorocarbon resist for high speed scanning probe lithography", *Angew. Chem.*, 2007, 46 (39), p. 7477–7480, 2007.
- [ROM 88] ROMIJN J., VAN DER DRIFT E., *Physica*, B 152, p. 14, 1988.
- [SAL 99] SALVAN F., THIBAUDAU F., "Microscopie à sonde locale", *Techniques de l'ingénieur, traité Analyse et caractérisation*, article no. P895, 1999.
- [SCH 98] SCHENK M., FUTING M., REICHELT R., "Direct Visualization of the Dynamic Behavior of a Water Meniscus by Scanning Electron Microscopy", *J. App. Phys.*, 84, p. 4880–4884, 1998.
- [SCH 03] SCHENKEL T., et al., "Solid state quantum computer development in silicon with single ion implantation" *J. Appl. Phys.*, 94, p.7017, 2003.
- [SCH 06] SCHENKEL, A TYRYSHKIN, M. DE SOUSA R., WHALEY K.B., BOKOR J., LIDDLE J.A., PERSAUD A., SHANGKUAN J., CHAKAROV I., LYON S. A., "Electrical activation and spin coherence of ultra low dose antimony implants in silicon", *Applied Physics Letters*, 88, p. 112101, 2006.
- [SHI 98] SHIRAKASHI J.I., MATSUMOTO K., MIURA N., KONAGAI M., "Single-electron charging effects in Nb/Nb oxide-based single-electron transistors at room temperature", *Appl. Phys. Lett.*, 72, p. 1893, 1998.
- [SOH 95] SOHN L.L., WILLETT R.L., "Fabrication of nanostructures using atomic-force-microscope-based lithography", *Appl. Phys. Lett.*, 67, p. 1552, 1995.
- [SNO 94] SNOW E.S., CAMPBELL P.M., "Fabrication of Si Nanostructures with an Atomic Force Microscope", *Applied Physics Letters*, 64, p. 1932–1934, 1994.
- [SNO 95] SNOW E.S., CAMPBELL P.M., "Afm Fabrication of Sub-10-Nanometer Metal-Oxide Devices with in Situ Control of Electrical Properties", *Science*, 270, p. 1639, 1995.
- [SNO 96] SNOW E.S., PARK D., CAMPBELL P.M., "Single-atom point contact devices fabricated with an atomic force microscope", *Appl. Phys. Lett.*, 69, p. 269, 1996.
- [STI 97] STIEVENARD D., FONTAINE P.A., DUBOIS E., "Nanooxidation Using a Scanning Probe Microscope: An Analytical Model Based on Field Induced Oxidation", *Applied Physics Letters*, 70, p. 3272–3274, 1997.
- [SYR 99] SYRYKH C., NYS J. P., LEGRAND B., STIÉVENARD D., "Nanoscale desorption of H-passivated Si(100)–2×1 surfaces using an ultrahigh vacuum scanning tunneling microscope", *J. Appl. Phys.*, 85, p. 3887, 1999.

- [TAB 92] TABATA O., ASAH I R., FUNABASHI H., SHIMAOKA K., SUGIYAMA S., “Anisotropic Etching of Silicon in Tmah Solutions”, *Sens. and Actuat.*, A 1, p. 51, 1992.
- [THI 94] THIBAUDAU F., ROCHE J.R., SALVAN F., “Nanometer-Scale Lithography on Si Surface by Decomposition of Ferrocene Molecules Using a Scanning Tunneling Microscope”, *Applied Physics Letters*, 64, p. 523–5, 1994.
- [TOR 03] TORRES C.M.S. (DIR.), *Alternative Lithography, Unleashing the Potentials of Nanotechnology*, Springer Technology & Industrial Arts, Berlin, 2003.
- [VET 00] P. VETTIGER, M. DESPONT, U. DRECHSLER, U. DÜRIG, W. HÄBERLE, M.I. LUTWYCHE, H.E. ROTHUIZEN, R. STUTZ, R. WIDMER & BINNIG G.K., “The ‘Millipede’: More Than One Thousand Tips for Future AFM Storage”, *IBM J. of Research and Development*, 44, p. 323, 2000.
- [VIL 04] VILLARROYA M., PEREZ-MURANO F., MARTIN C., DAVIS Z., BOISEN A., ESTEVE J., FIGUERAS E., MONTSERRAT J., BARNIOL N., “AFM lithography for the definition of nanometre scale gaps: application to the fabrication of a cantilever-based sensor with electrochemical current detection”, *Nanotechnology*, 15, p. 771–776, 2004.
- [WAD 01] WADU-MESTHRIGE K., AMRO N.A., GARNO J.C., XU S., LIU G.Y., “Fabrication of Nanometer-Sized Protein Patterns Using Atomic Force Microscopy and Selective Immobilization”, *Biophys. J.*, vol. 80, p. 1891–1899, 2001.
- [WIE 94] WIESENDANGER R., *Scanning Probe Microscopy and Spectroscopy, Methods and Applications*, Cambridge University Press, Cambridge, USA, 1994.
- [WIL 97] WILDER K., SOH HYONGSOK T., ATALAR A., QUATE C.F., “Hybrid atomic force/scanning tunneling lithography”, *J. Vac. Sci. Technol.*, B 15, n° 5, p. 1811–1817, 1997.
- [WIL 98]. WILDE K, QUATE C. F., SINGH B., KYSER D.F., “Electron beam and scanning probe lithography: A comparison”, *J. Vac. Sci. Technol.*, B 6, p. 3864, 1998.